Supporting Information

Coumarin-Tethered 1,2,3-Triazole Based Fluorescent "Turn-ON" Probe via Metal-Free Click Chemistry for Selective Sensing of Serum Albumin: Quantitative Detection of HSA in Urine

Juheli Sadhukhan, Pabitra Mandal, Susanta Sekhar Adhikari*, Smritimoy Pramanik*

Department of Chemistry, University of Calcutta, 92 A.P.C. Road, Kolkata 700 009, India

*Corresponding author E-mail: adhikarisusanta@yahoo.com/ ssachem@caluniv.ac.in, spchem@caluniv.ac.in

1. ^{1}H and ^{13}C NMR of compounds

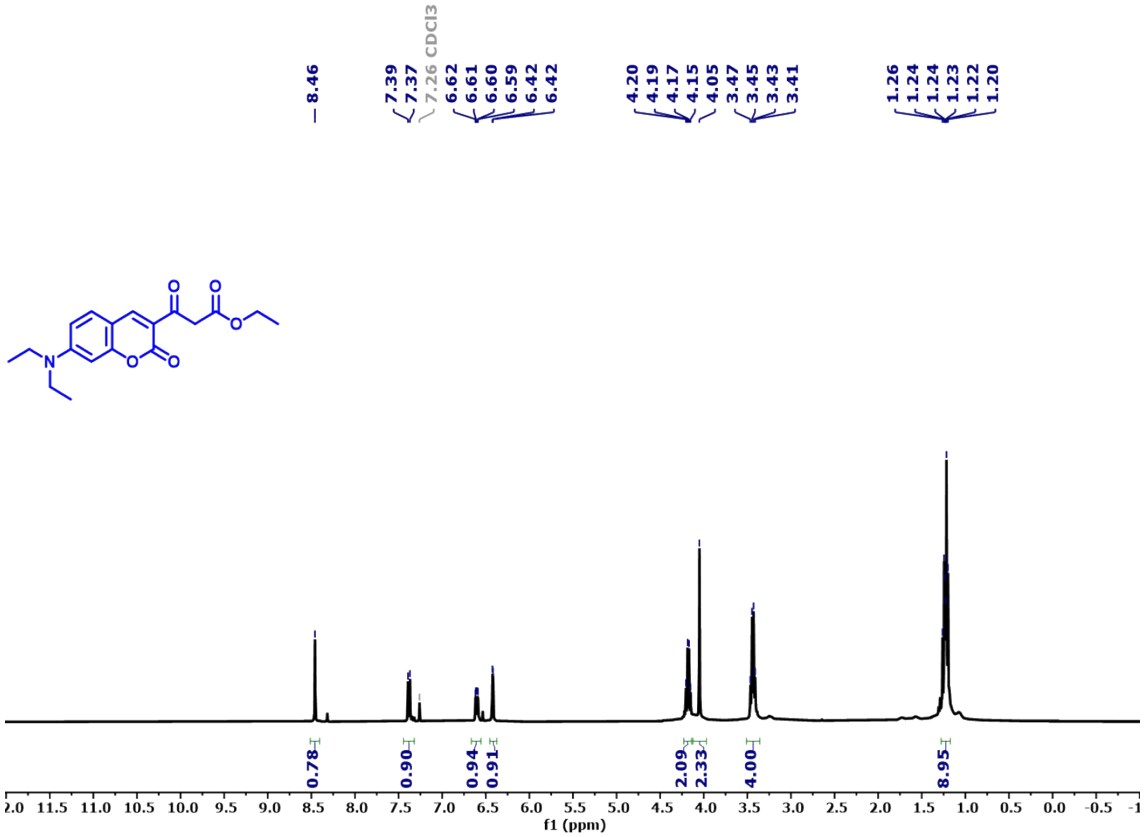

Fig. S1. ^{1}H NMR of compound **1** in $CDCl_3$ (400 MHz)

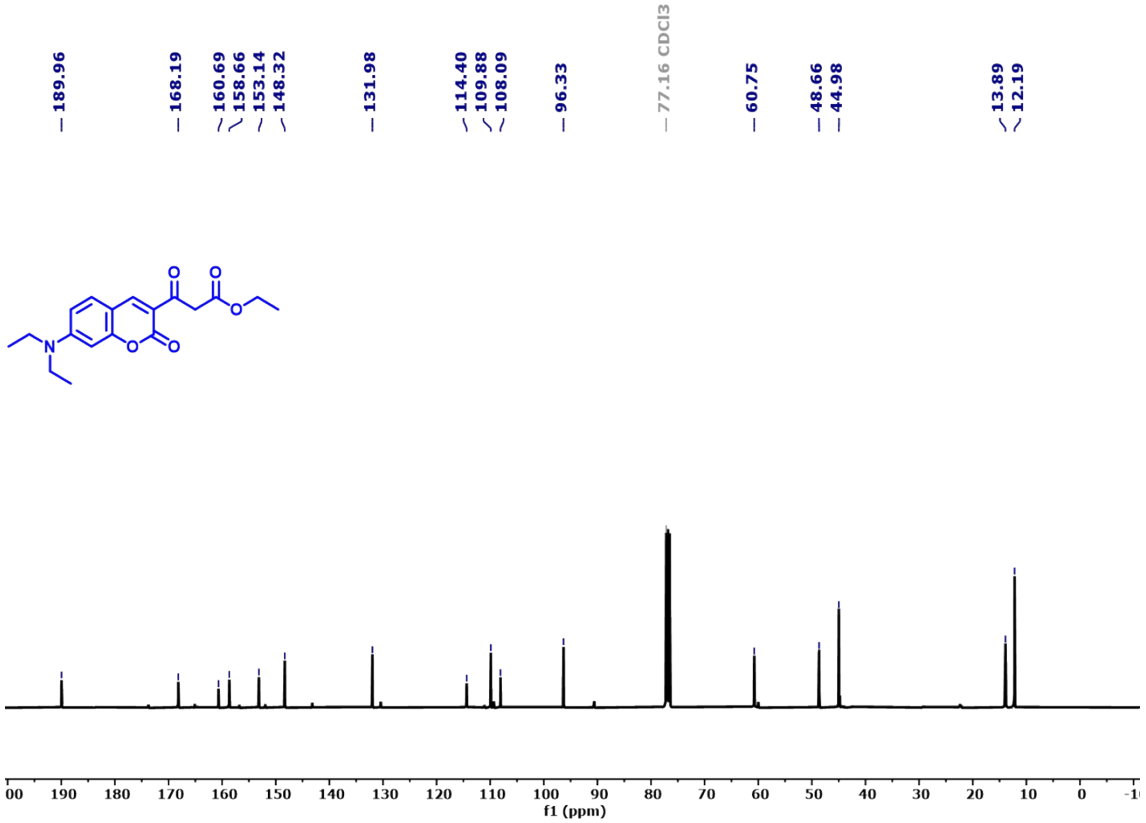

Fig. S2. ^{13}C NMR of compound **1** in $CDCl_3$ (100 MHz)

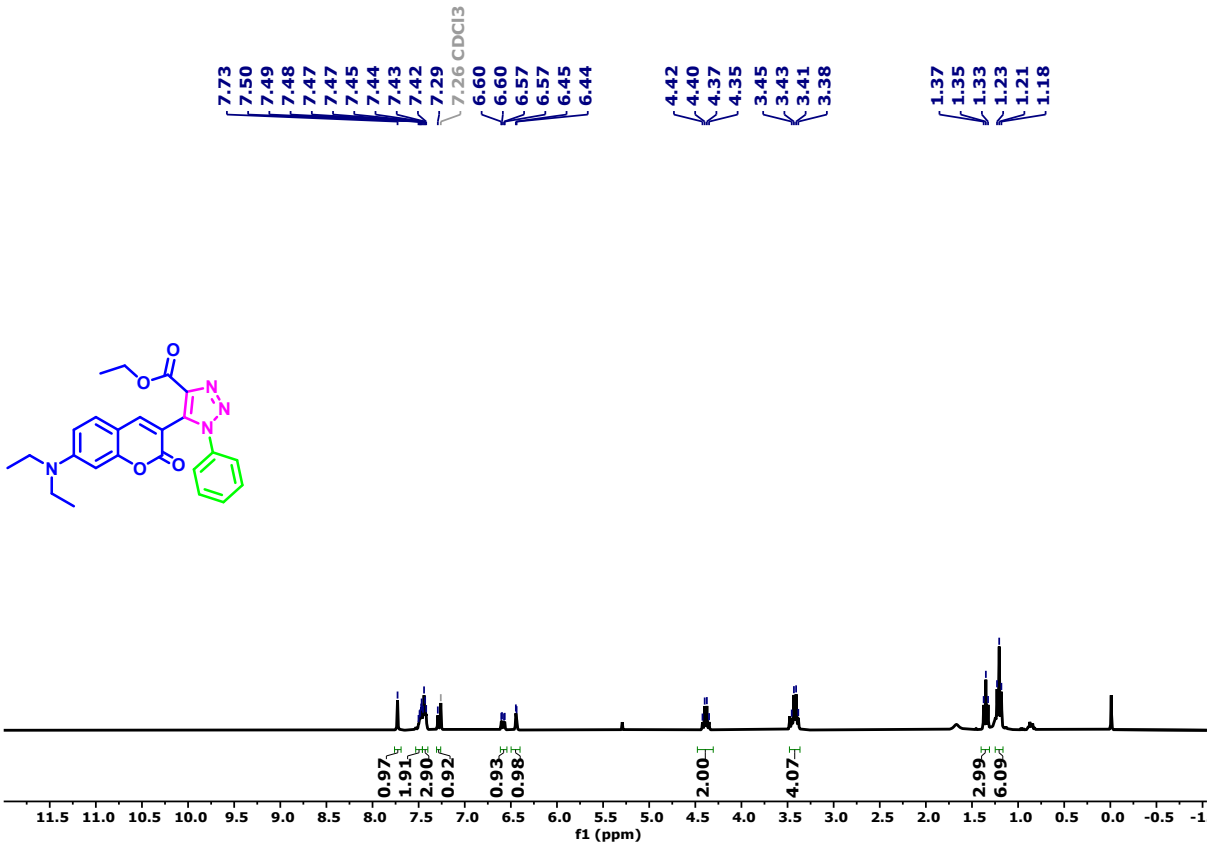

Fig. S3. ^{1}H NMR of compound **3a** in $CDCl_3$ (300 MHz)

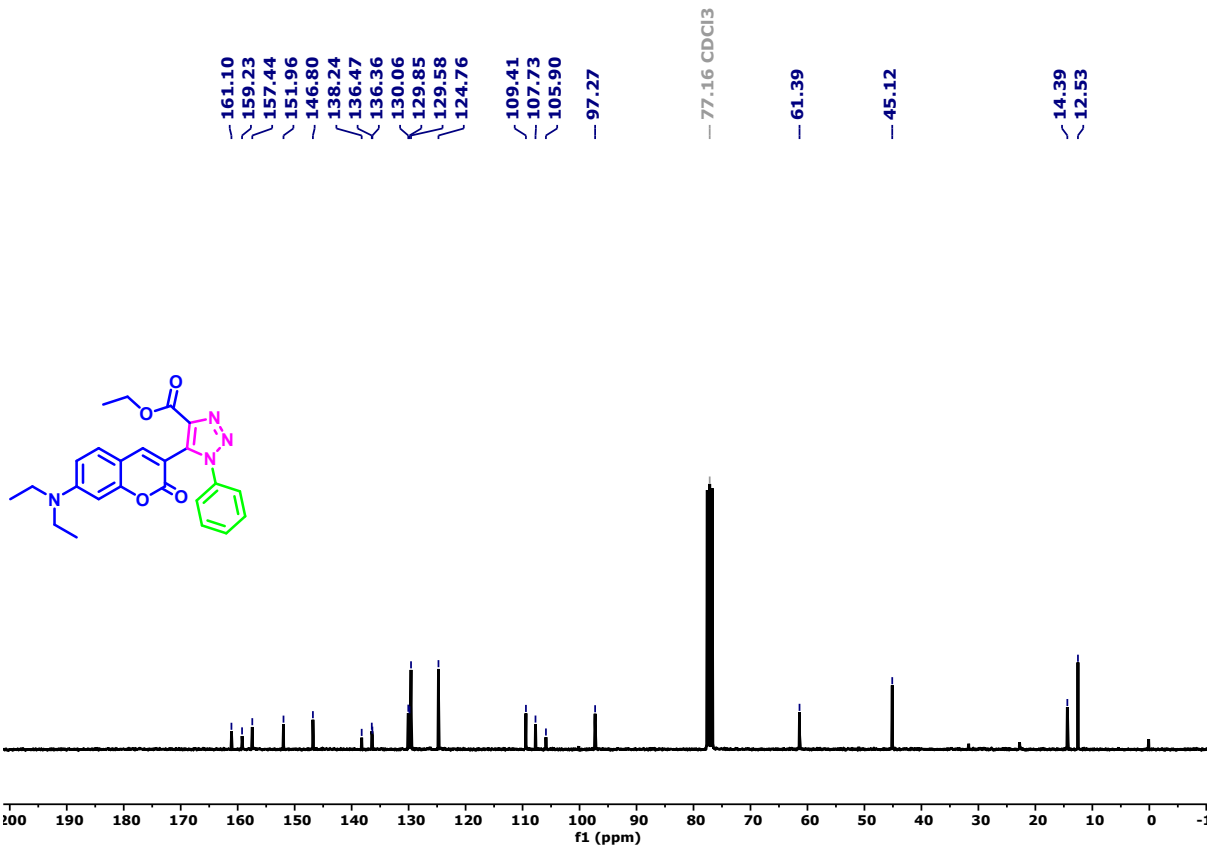

Fig. S4. ^{13}C NMR of compound **3a** in $CDCl_3$ (75 MHz)

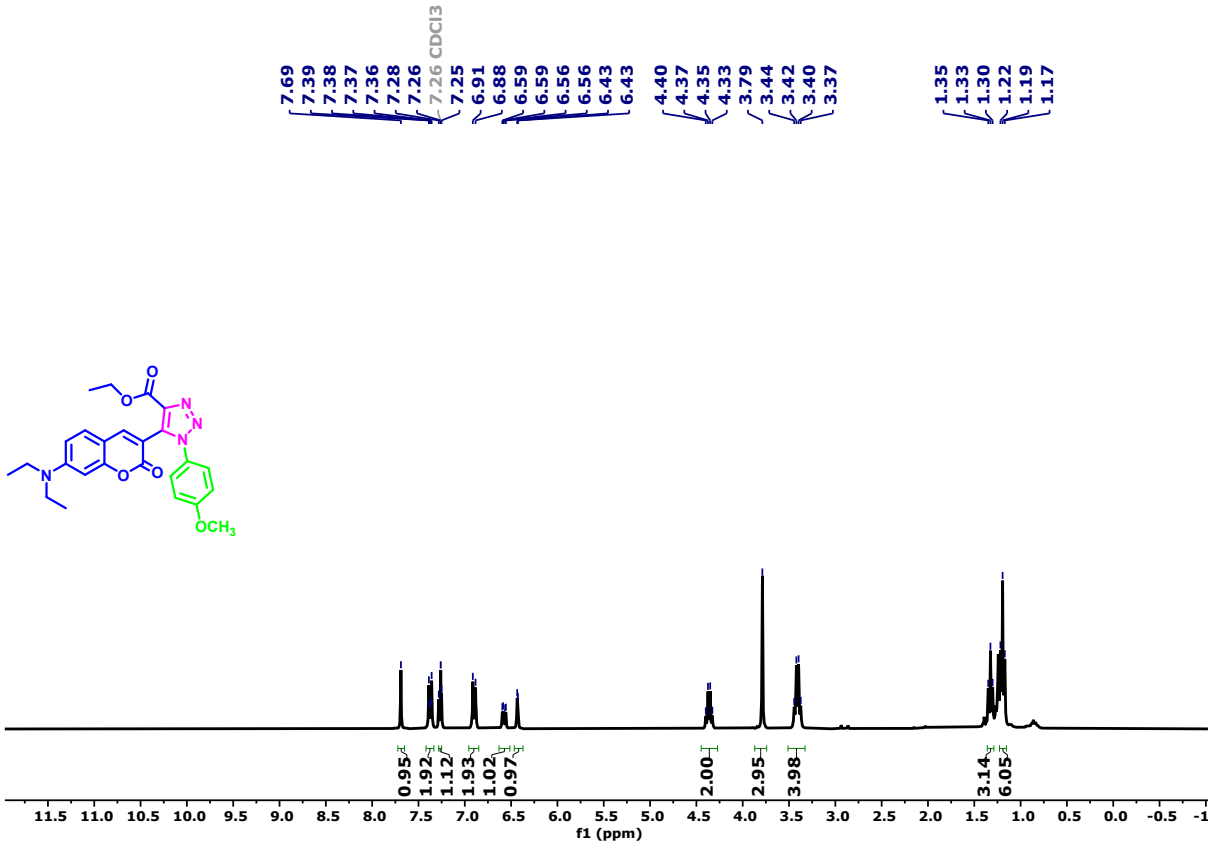

Fig. S5. ^{1}H NMR of compound **3b** in $CDCl_3$ (300 MHz)

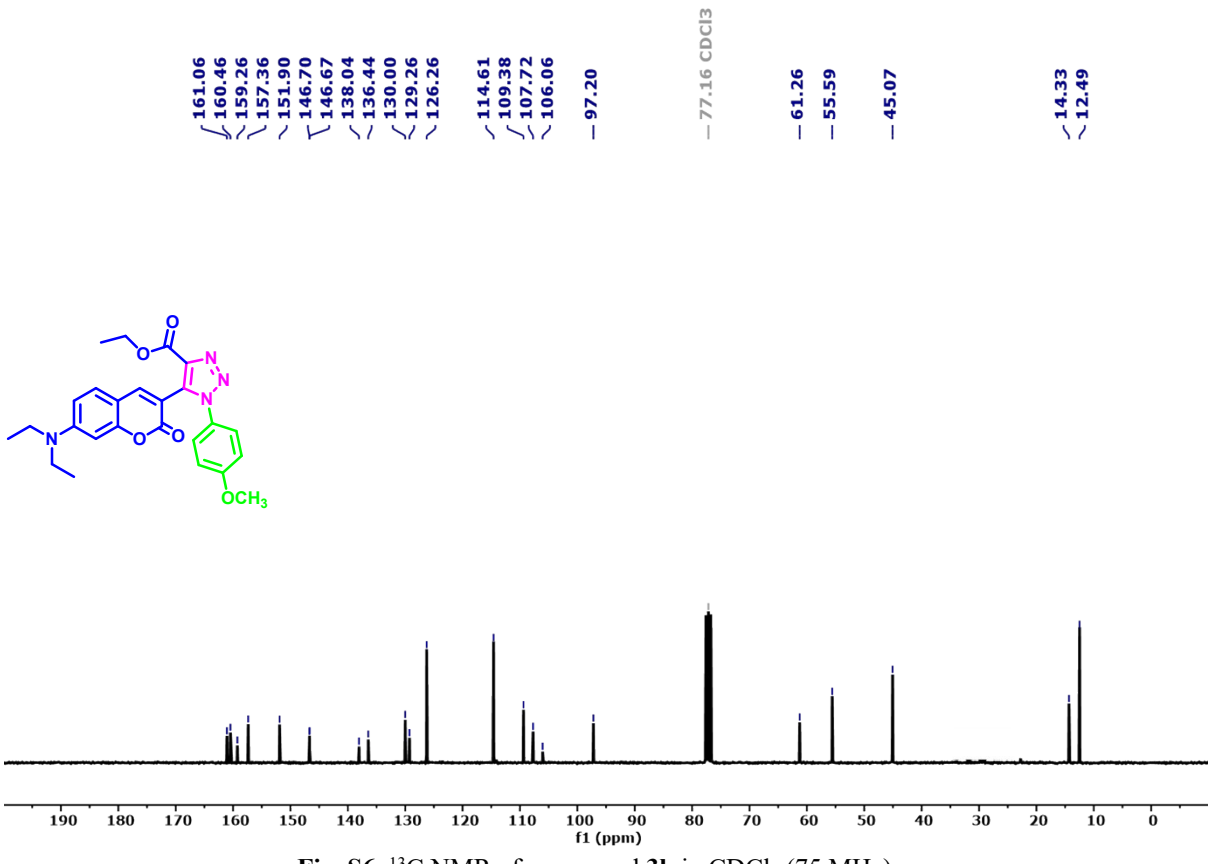

Fig. S6. ^{13}C NMR of compound **3b** in $CDCl_3$ (75 MHz)

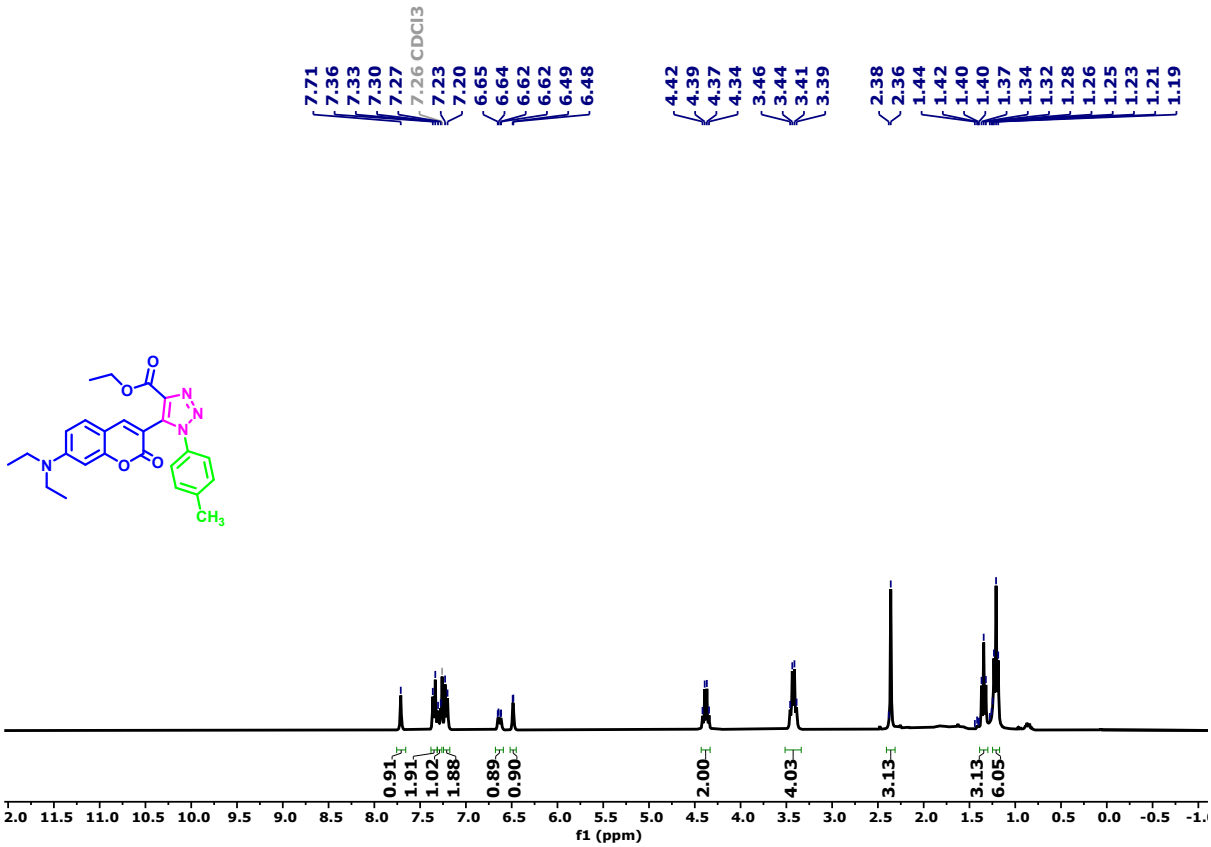

Fig. S7. ^{1}H NMR of compound **3c** in $CDCl_3$ (300 MHz)

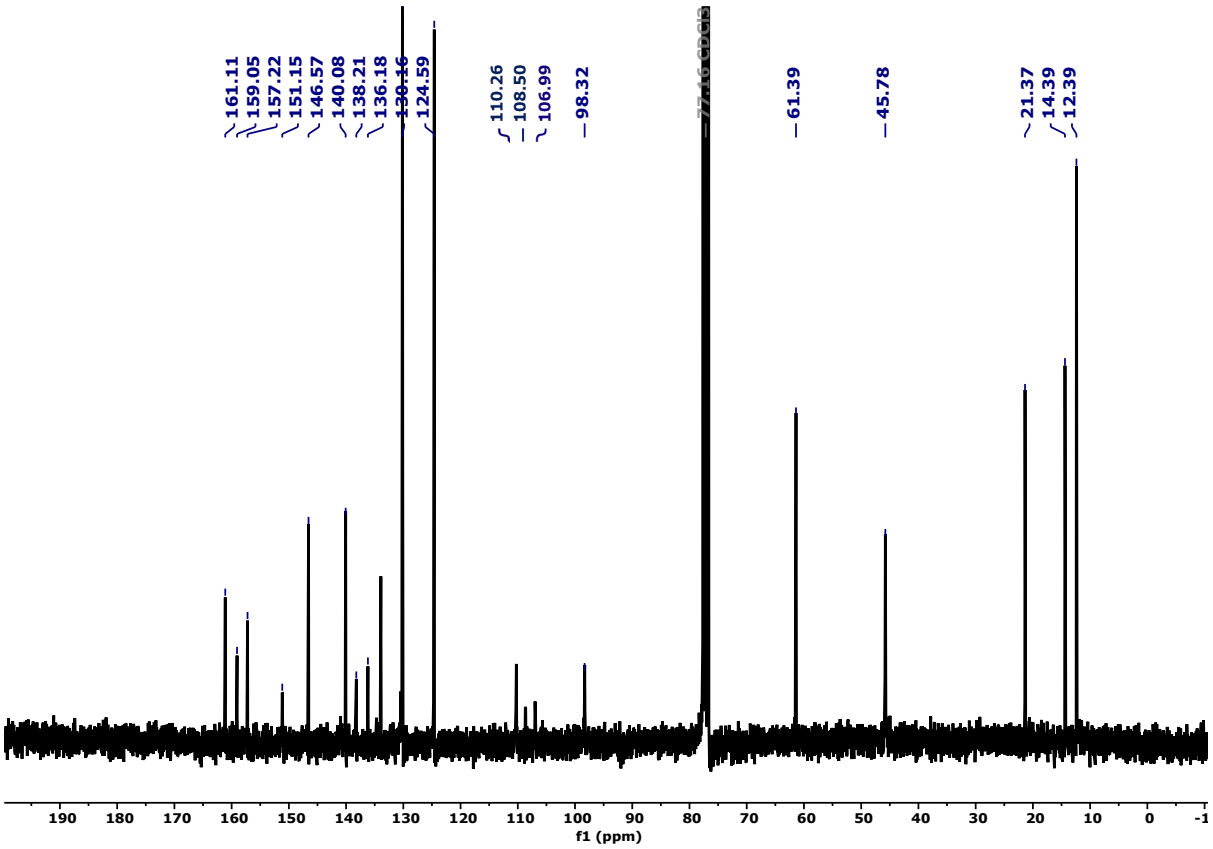

Fig. S8. ^{13}C NMR of compound **3c** in $CDCl_3$ (75 MHz)

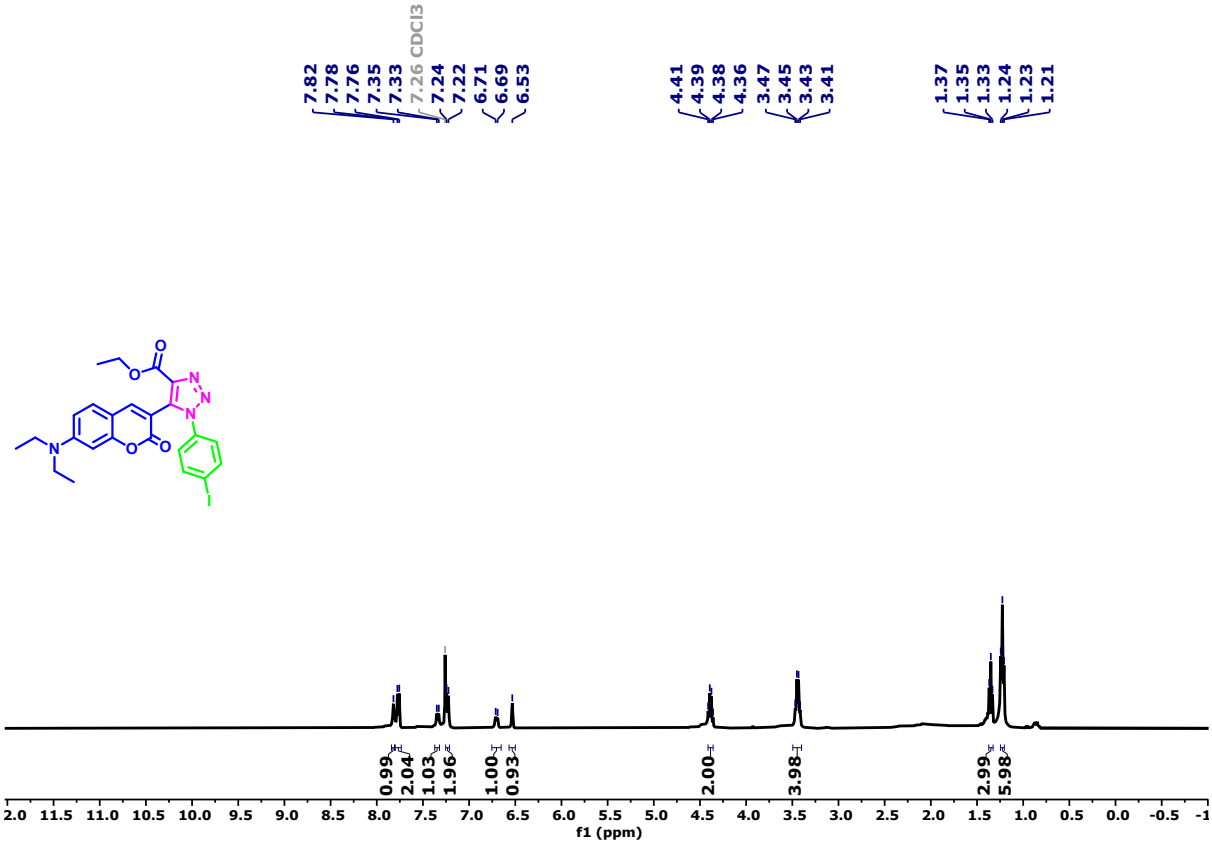

Fig. S9. ^{1}H NMR of compound **3d** in $CDCl_3$ (400 MHz)

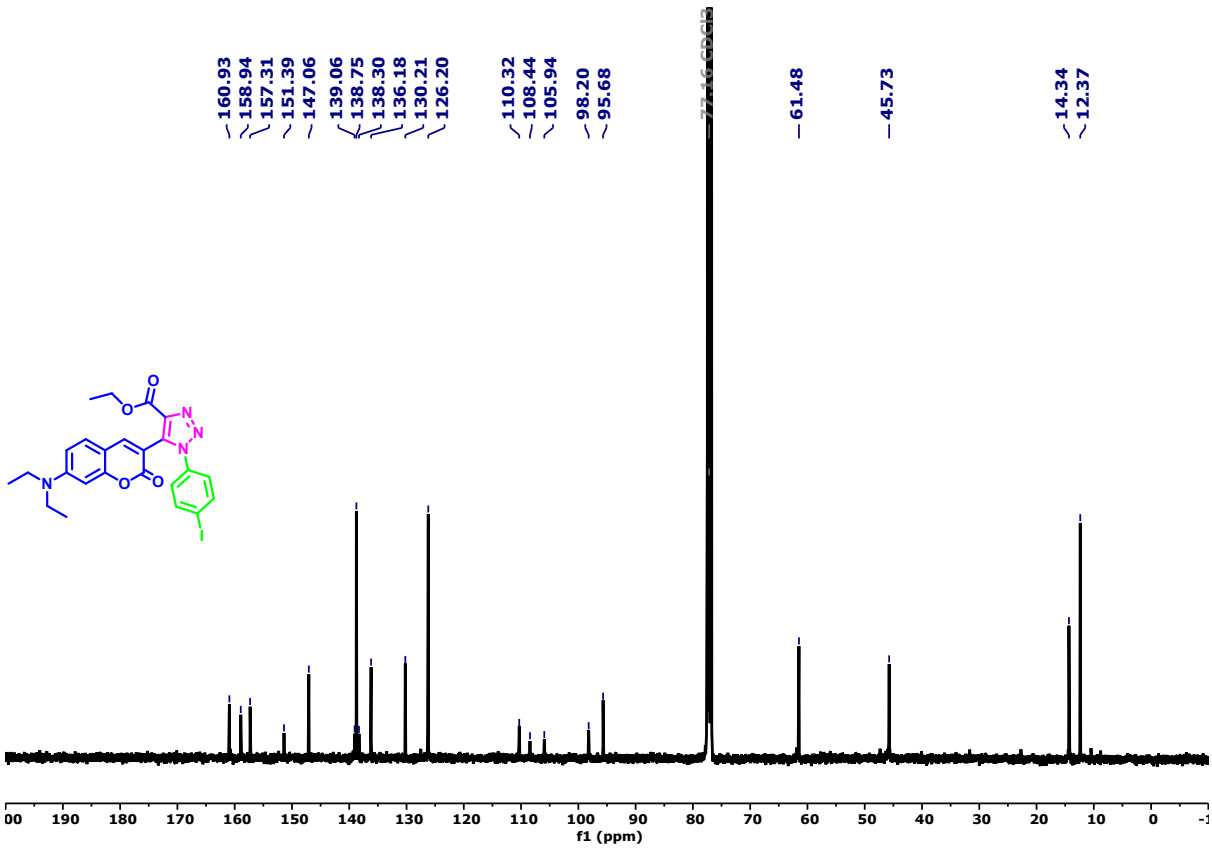

Fig. S10. ^{13}C NMR of compound **3d** in $CDCl_3$ (100 MHz)

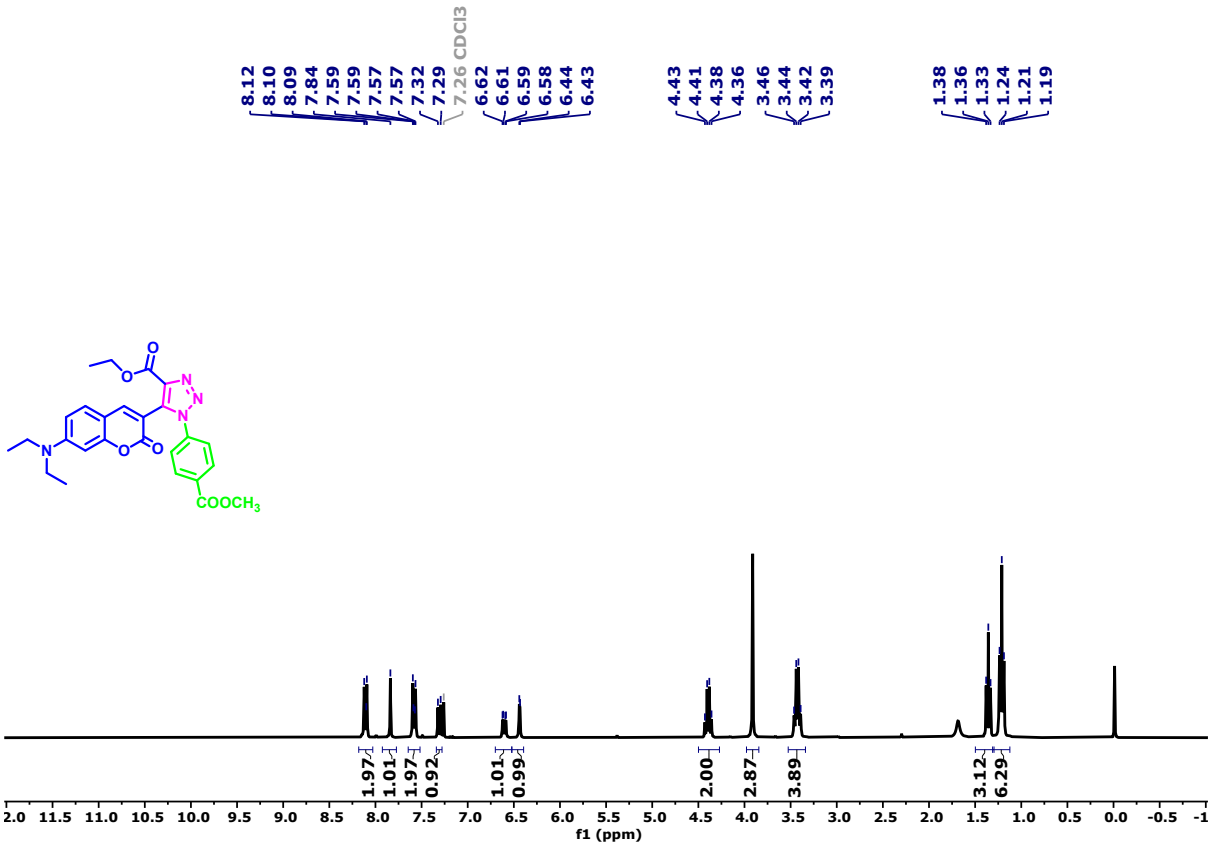

Fig. S11. ^{1}H NMR of compound **3e** in $CDCl_3$ (300 MHz)

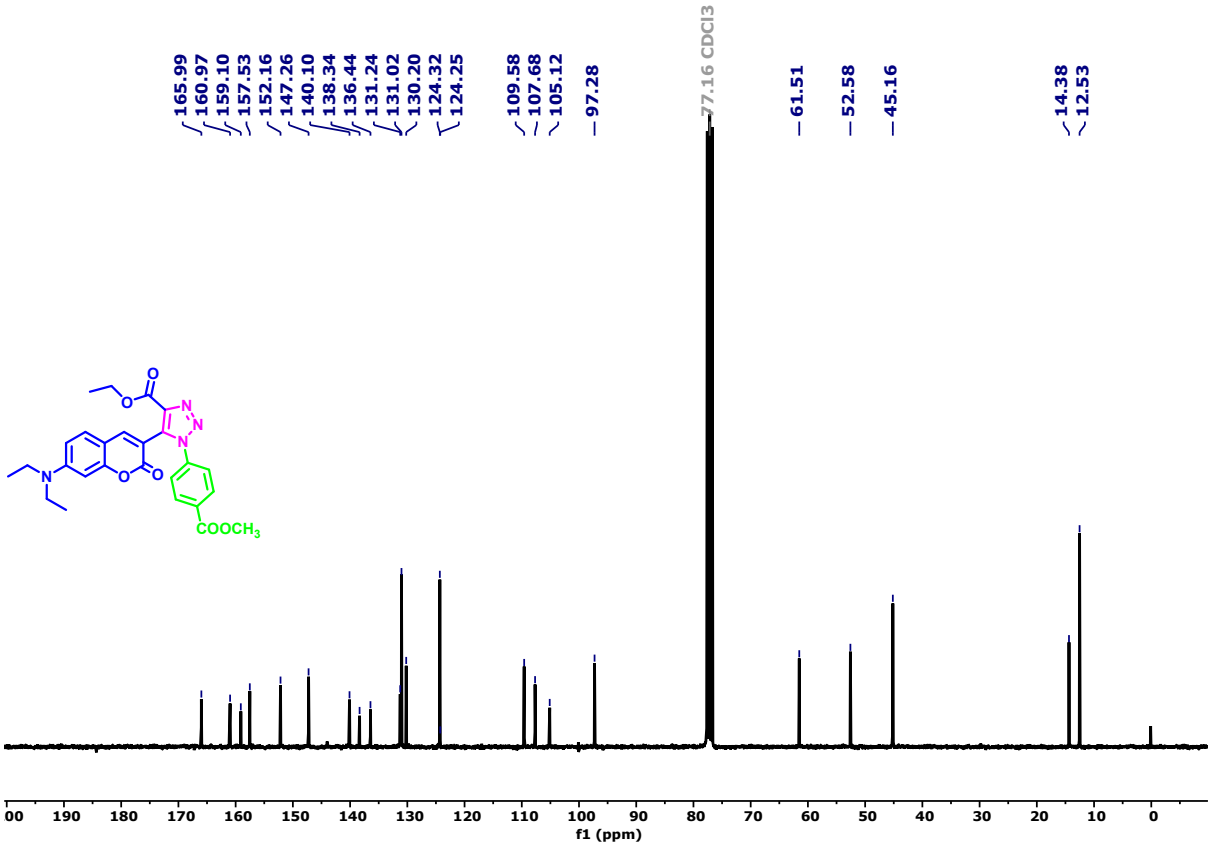

Fig. S12. ^{13}C NMR of compound **3e** in $CDCl_3$ (75 MHz)

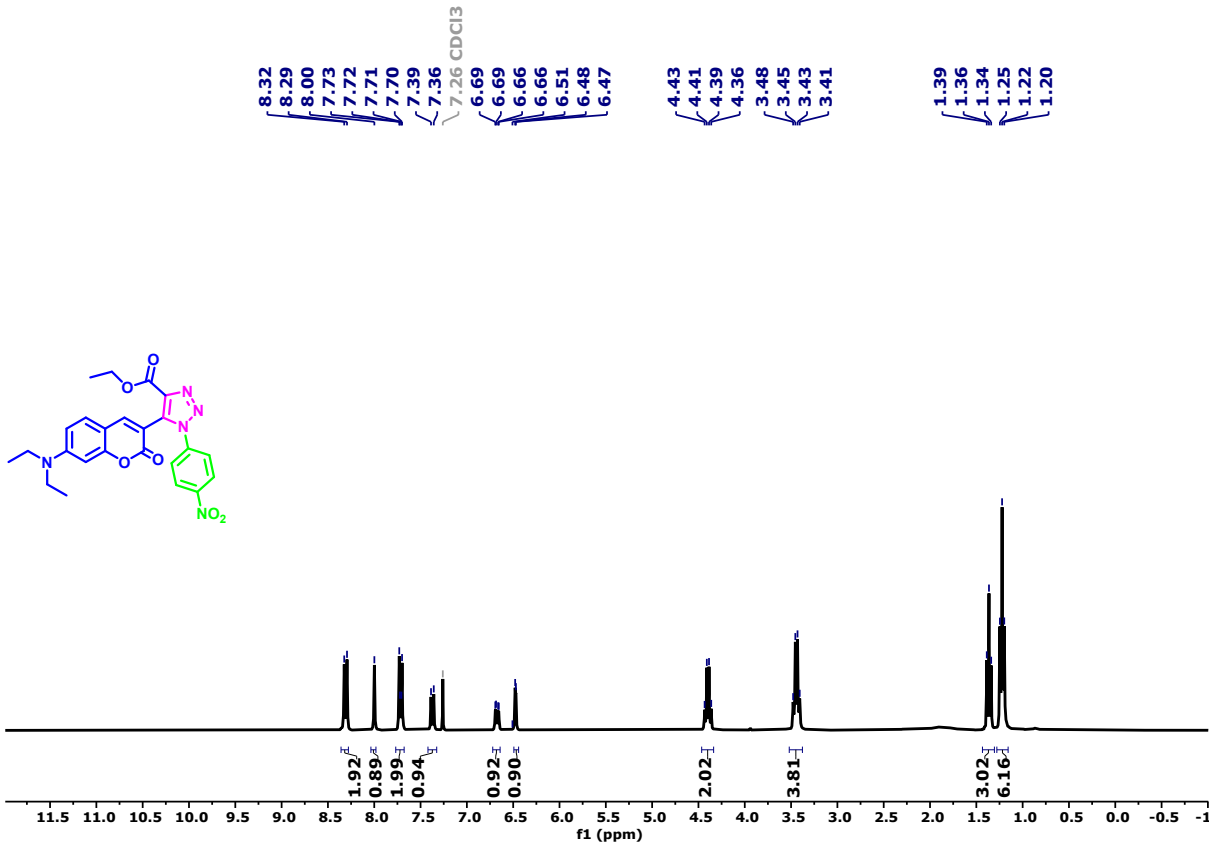

Fig. S13. ^{1}H NMR of compound **3f** in $CDCl_3$ (300 MHz)

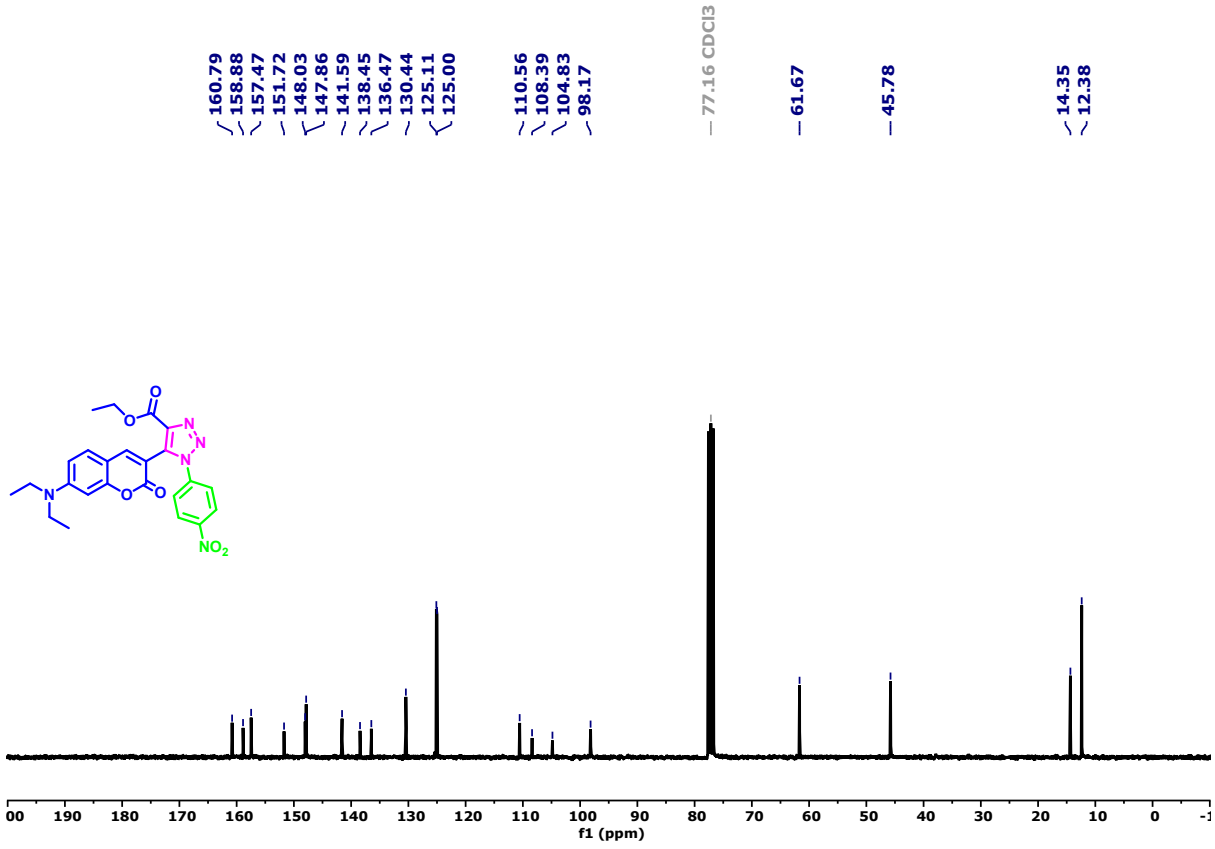

Fig. S14. ^{13}C NMR of compound **3f** in $CDCl_3$ (75 MHz)

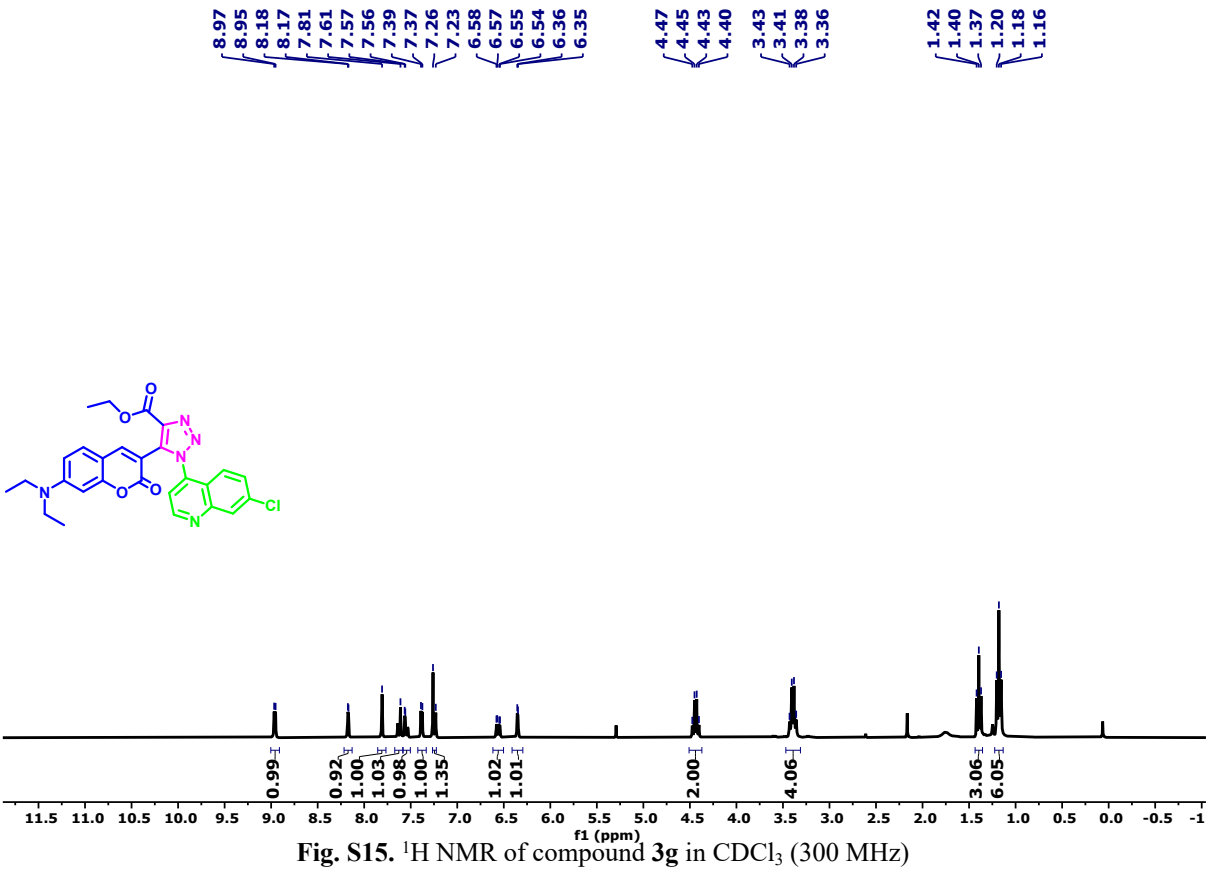

Fig. S15. ^{1}H NMR of compound **3g** in $CDCl_3$ (300 MHz)

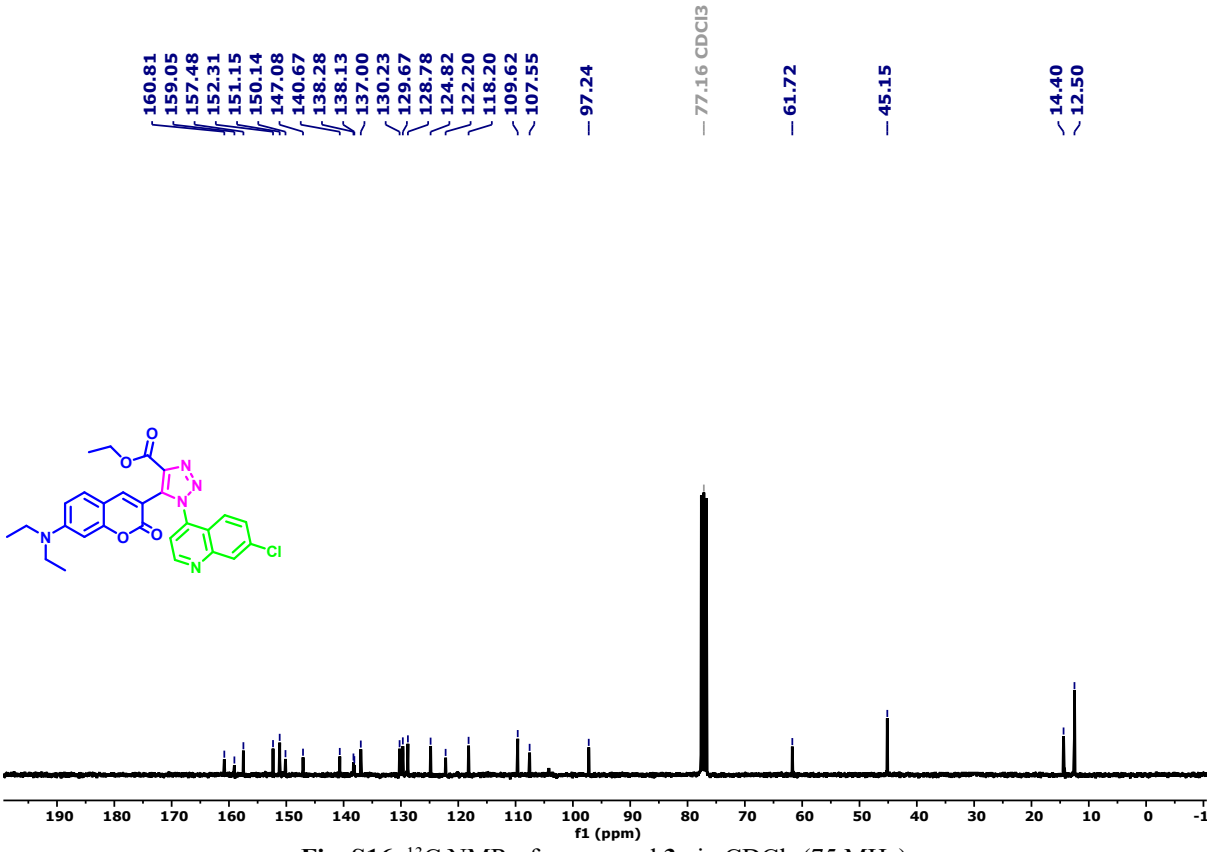

Fig. S16. ^{13}C NMR of compound **3g** in $CDCl_3$ (75 MHz)

2. Photophysical Studies of the compounds (3a-e) and 3g

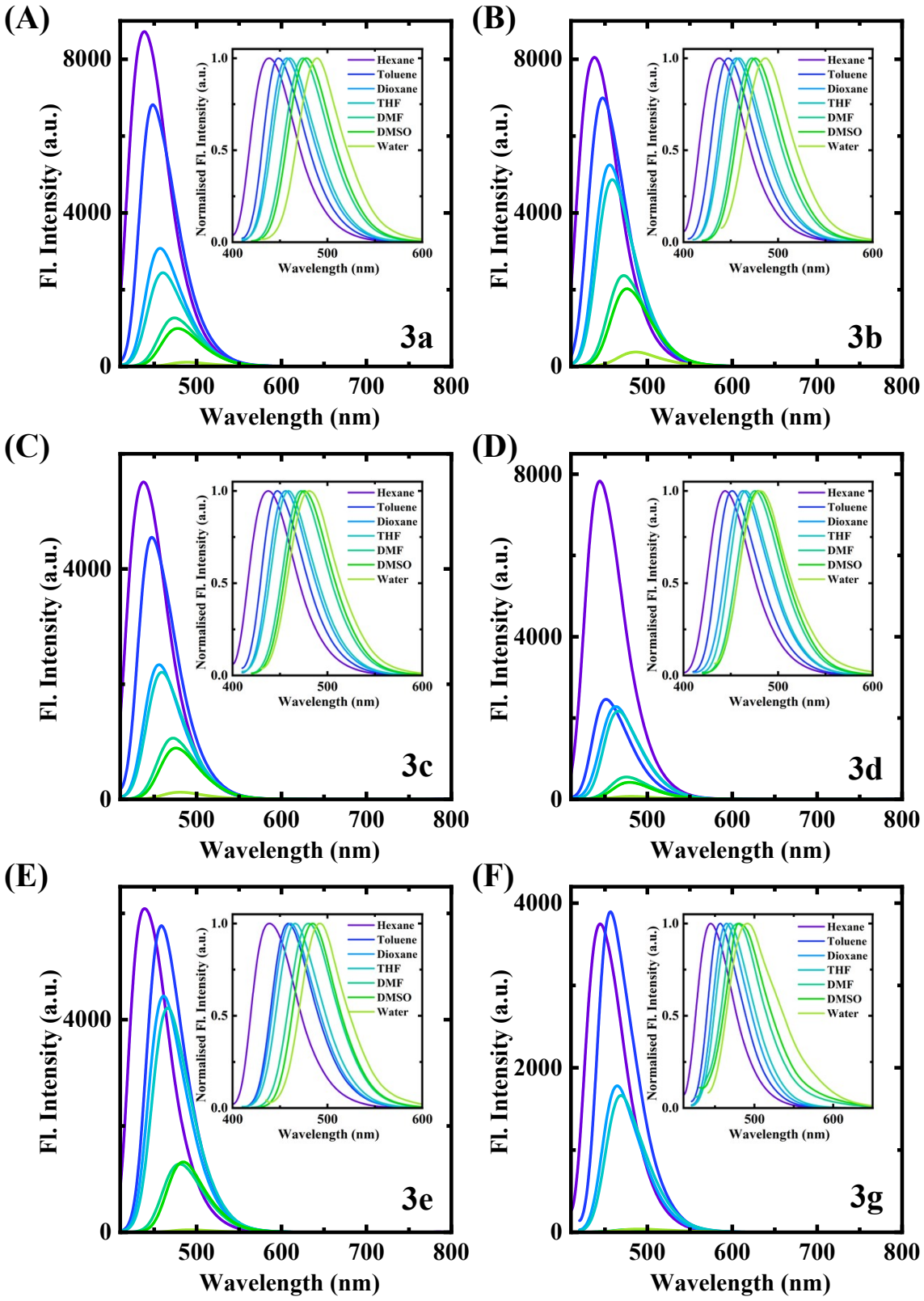

Fig. S17. Fluorescence emission spectra of compounds **3a-e** and **3g** in solvents of different polarities.

2. Absorption spectra of compounds (3a-e) and 3g

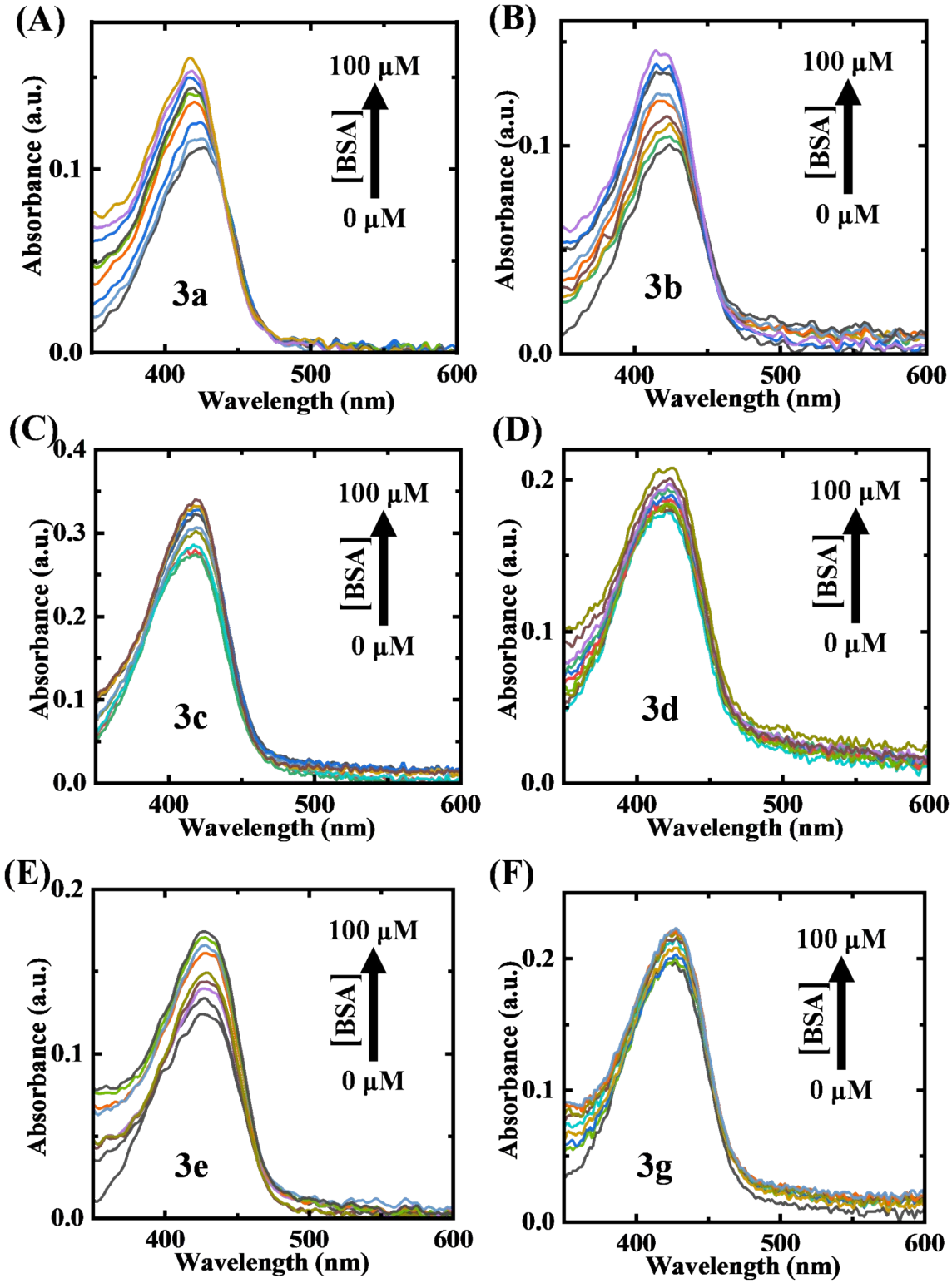

Fig. S18. Absorption spectra of compounds **3a-e** and **3g** upon addition of 1 to 100 μM BSA.

3. **Emission spectra of compounds (3a-e) and 3g**

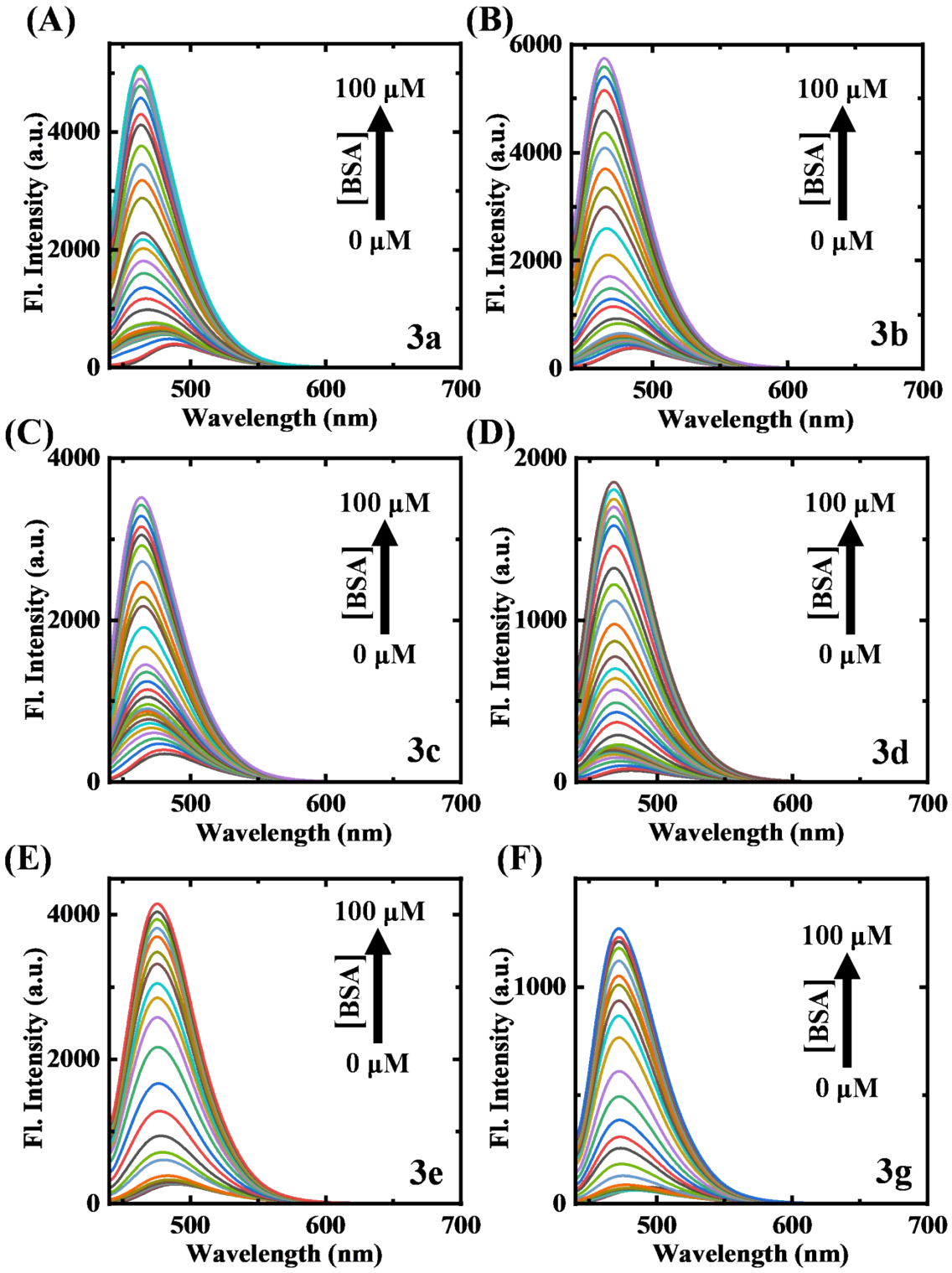

Fig. S19. Emission spectra of compounds **3a-e** and **3g** upon addition of 1 to 100 µM BSA.

4. Estimation of the binding constants of compounds (3a-e) and 3g

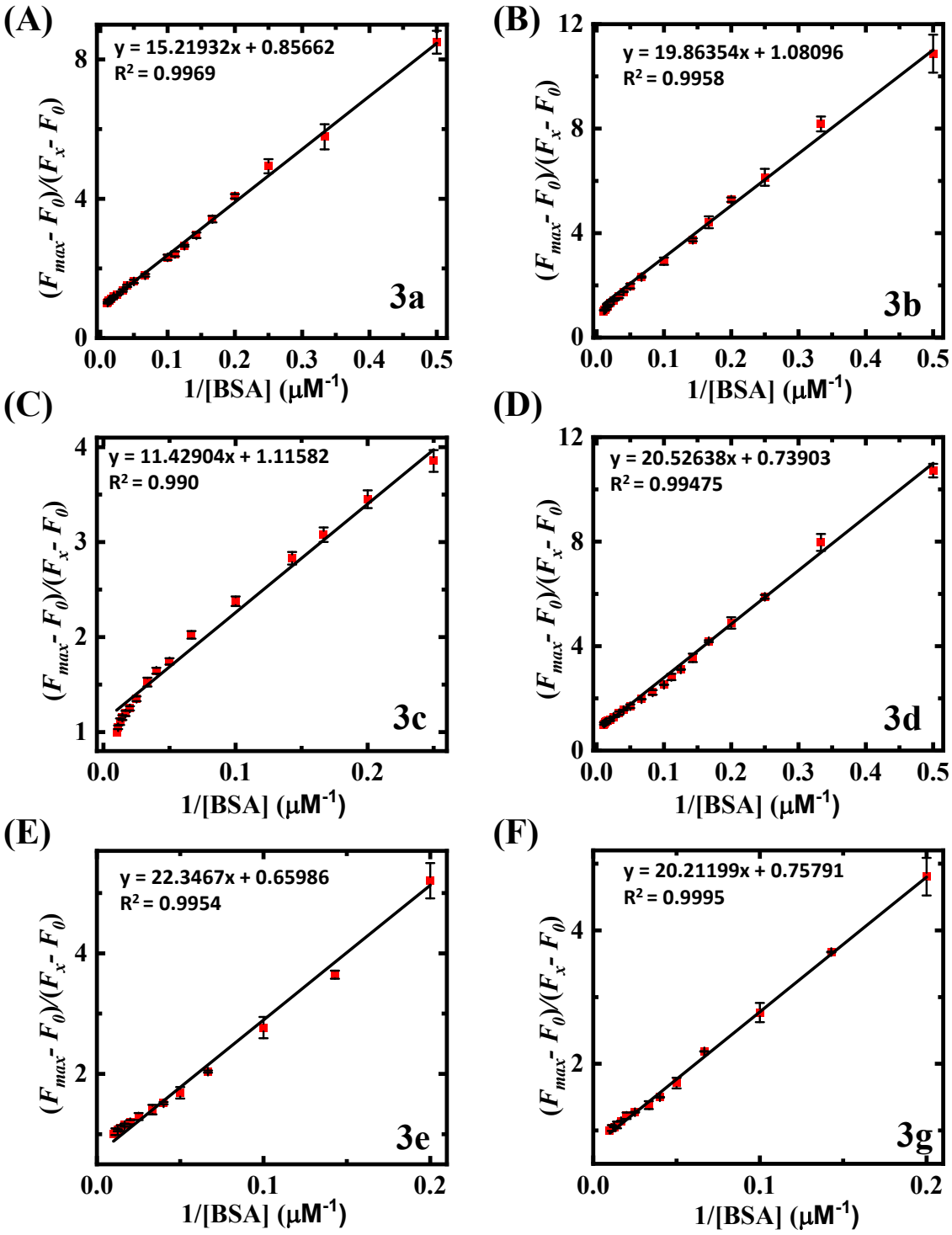

Fig. S20. Benesi-Hildebrand plot of compounds **3a-e** and **3g** upon addition of BSA. Error bars: (±SD, n=3).

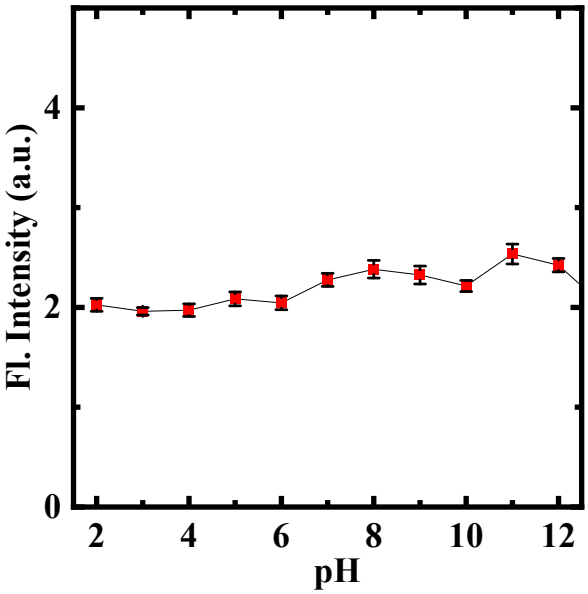

Fig. S21. Fluorescence intensity linear plot of probe **3f** in pH range 2–12. Error bars: (±SD, n=3).

5. pH sensitivity of the probe 3f

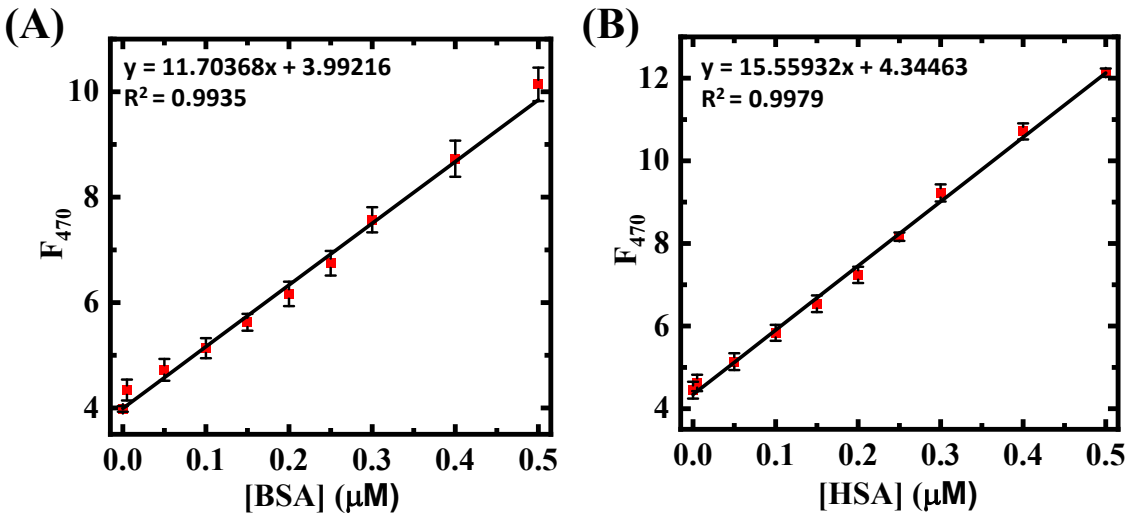

Fig. S22. (A) Linear plot of emission intensity vs. concentration of BSA and (B) concentration of HSA. Error bars: (±SD, n=3).

6. Limit of Detection of probe 3f for BSA and HSA sensing

Calculation:

To determine the detection limit of **3f** for both BSA and HSA, fluorescence intensities of **3f** were recorded upon addition of 0 to 0.5 μM BSA and HSA. Then the LOD value was calculated using the following equation

LOD = 3σ/s = 0.18/ (11.70 X 10^{-6} M^{-1}) = 15.4 nM

where σ is the standard deviation of blank measurement, and s is the slope between the fluorescence emission intensity at 470 nm versus the concentration of BSA.

Similarly, for HSA, s = 15.57 X 10^{-6} M^{-1}, the LOD value calculated is 11.6 nM.

The limit of quantification (LOQ) values of **3f** for both BSA and HSA were also calculated by using the equation LOQ = 10σ/s. The LOQ values were found to be 51.3 nM and 38.6 nM, for BSA and HSA, respectively.

5. Table S1: Comparison with other small molecule donor–π–acceptor probes for the detection of human serum albumins

Sl. No.	Structure	LOD	Reference
1.	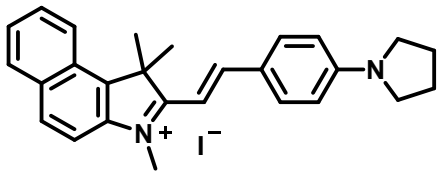	3.44 μM	*J. Lumin.*, 2017, **192**, 478–485.
2.	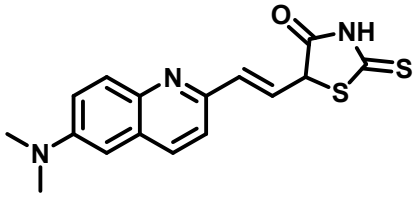	18.1 nM	*Sens. Actuators, B*, 2018, **271**, 82–89.
3.	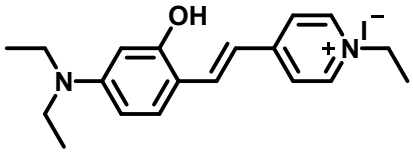	4.8 nM	*Spectrochim. Acta, Part A*, 2019, **223**, 117318.
4.	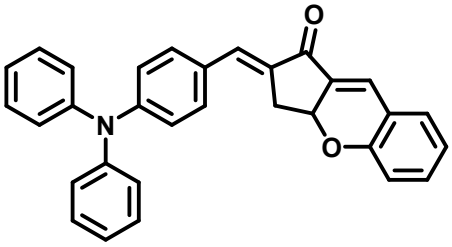	30.9 μM	*Spectrochim. Acta, Part A*, **2021**, *250*, 119409.

5.	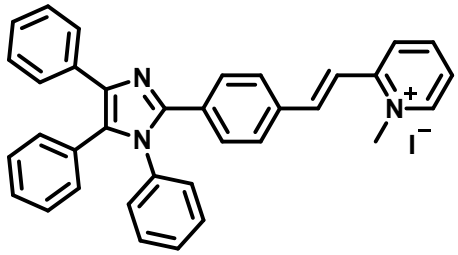	0.06 µM	*Bioorg. Med. Chem. Lett.*, 2021, **53**, 128438.
6.	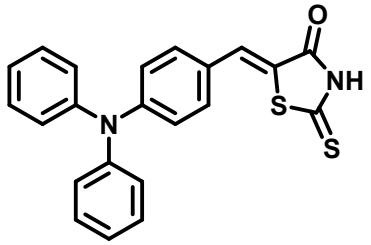	2.52 µM	*Anal. Chim. Acta,* 2022*,* **1190**, 339267.
7.	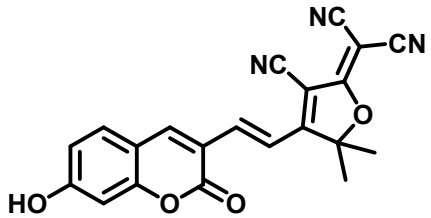	3.5 µM	*Chin. Chem. Lett.*, 2023, **34**, 107557.
8.	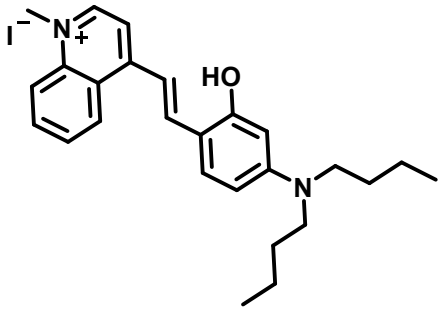	2.39 nM	*J. Mater. Chem. B*, 2024, **12**, 8791.
9.	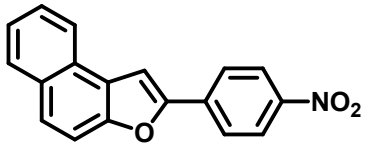	0.24 µM	*Chem Asian J.,* 2024, **19**, e202301055
10.	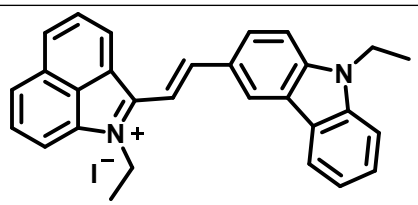	14.7 nM	*Spectrochim. Acta, Part A*, 2026, **352**, 127503.
11.	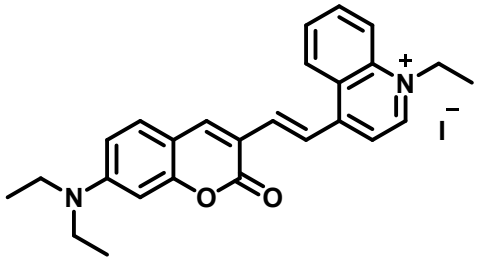	0.97 µM	*Biosens. Bioelectron.*, 2026, **301**, 118490.

12.	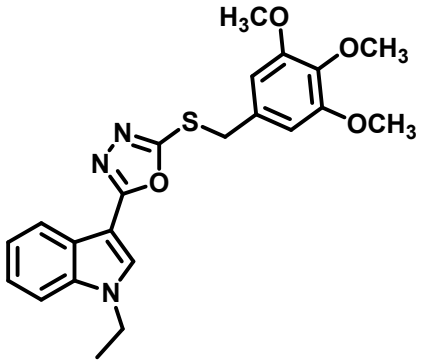	0.47 µM	*Anal. Biochem.*, 2026, **713**, 116090.
13.	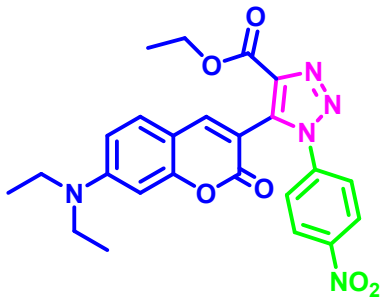	11.6 nM	*This work*

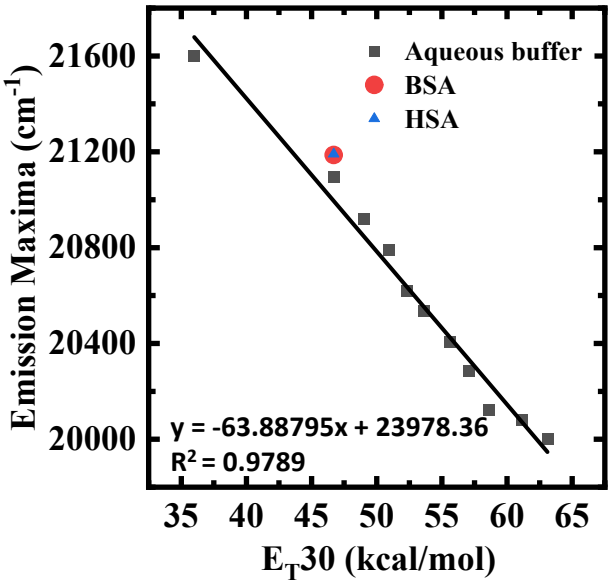

Fig. S23. Variation of energy corresponds to the emission maxima of **3f** as a function of E_T (30) in a water-dioxan mixture. The interpolated value corresponds to the **3f** in the BSA (blue) and HSA (red) environment.

7. Micropolarity Analysis of Probe 3f within the Protein Binding Pocket

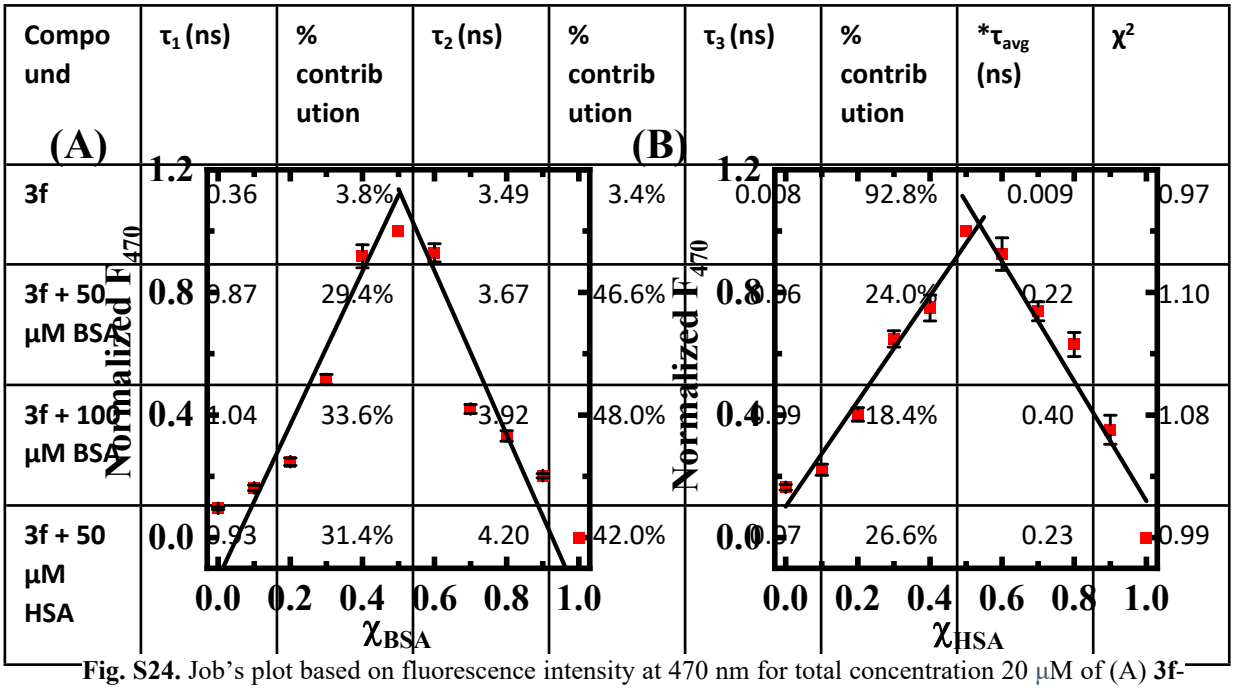

Compound	τ_1 (ns)	% contribution	τ_2 (ns)	% contribution	τ_3 (ns)	% contribution	$*\tau_{avg}$ (ns)	χ^2
3f	0.36	3.8%	3.49	3.4%	0.008	92.8%	0.009	0.97
3f + 50 µM BSA	0.87	29.4%	3.67	46.6%	0.06	24.0%	0.22	1.10
3f + 100 µM BSA	1.04	33.6%	3.92	48.0%	0.09	18.4%	0.40	1.08
3f + 50 µM HSA	0.93	31.4%	4.20	42.0%	0.07	26.6%	0.23	0.99

Fig. S24. Job's plot based on fluorescence intensity at 470 nm for total concentration 20 µM of (A) **3f**-BSA and (B) **3f**-HSA in a buffer containing 10 mM Na_2HPO_4 (pH = 7.4) at 25 °C. Error bars: (±SD, n=3).

8. Job's plot for BSA and HSA

9. Table S2: Time-resolved fluorescence analysis decay parameters of 3f in absence and presence of BSA and HSA

3f + 100 µM HSA	1.33	39.0%	4.83	35.7%	0.124	25.3%	0.42	0.95
*Estimated errors within ±5%.								

10. Table S3: Secondary structure analysis (infrared spectra) for the free BSA and HSA and their corresponding complexes with 3f

Amide I (cm^{-1}) components	**BSA (500 µM)**	**BSA+ 3f (500µM+ 500µM)**	**HSA (500 µM)**	**HSA + 3f (500µM+ 500µM)**
α-helix 1650–1660	54% (1650)	38% (1650)	62% (1650)	43% (1650)
β-sheet 1614–1637	17% (1614, 1623)	14% (1613, 1624)	19% (1611, 1624)	15% (1613, 1623)
random coil 1638–1648	10% (1640)	28% (1640)	8% (1640)	27% (1640)
β-turn 1660–1680	16% (1675)	14% (1675)	9% (1678)	10% (1675)
β-antiparallel 1680–1692	5% (1687)	6% (1688)	2% (1690)	5% (1688)

11. Table S4: Comparison of α-helix content from FT-IR and CD spectroscopy

Compound	**% α-helix (FT-IR)**	**% α-helix (CD)**
BSA	54%	56%
BSA + 3f (1:1)	38%	39%
HSA	62%	61%
HSA + 3f (1:1)	43%	44%

12. Site-Marker Study

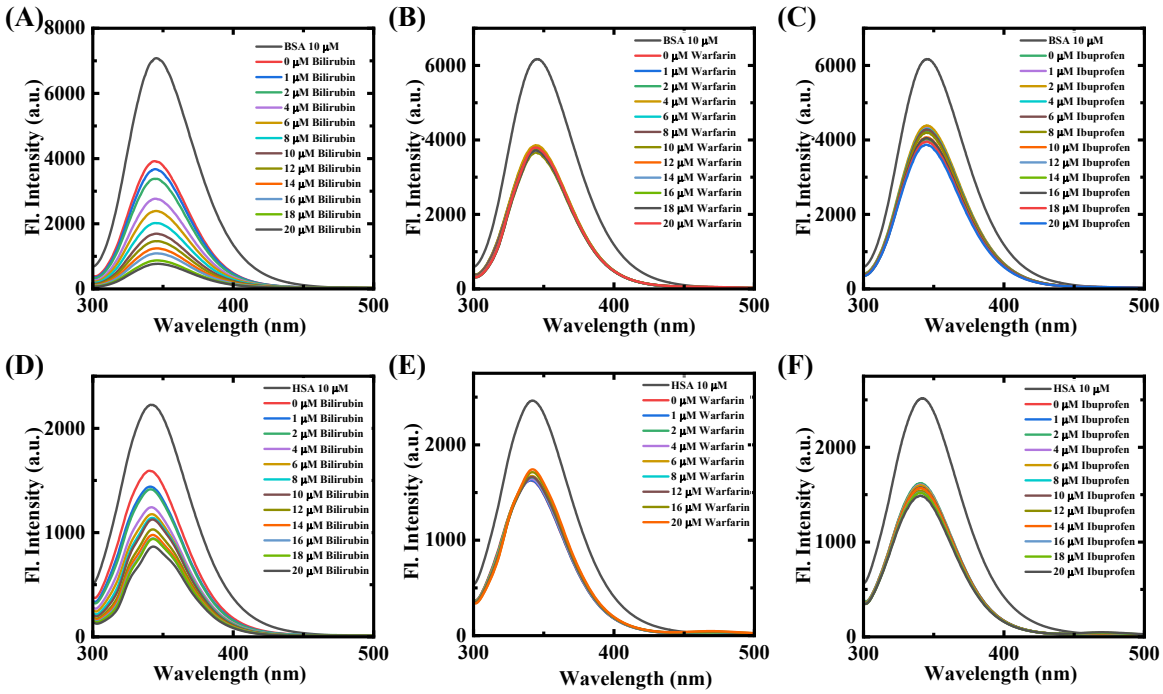

Fig. S25. Emission intensity of the 10μM [BSA-**3f**] complex and [HSA-**3f**] complex in the presence of increasing concentration of the bilirubin (A, D), warfarin (B, E), ibuprofen (C, F) [0-20 μM, (0-2eq)] in a buffer containing 10 mM Na_2HPO_4 (pH = 7.4) at 25 °C. λ_{ex} = 290 nm

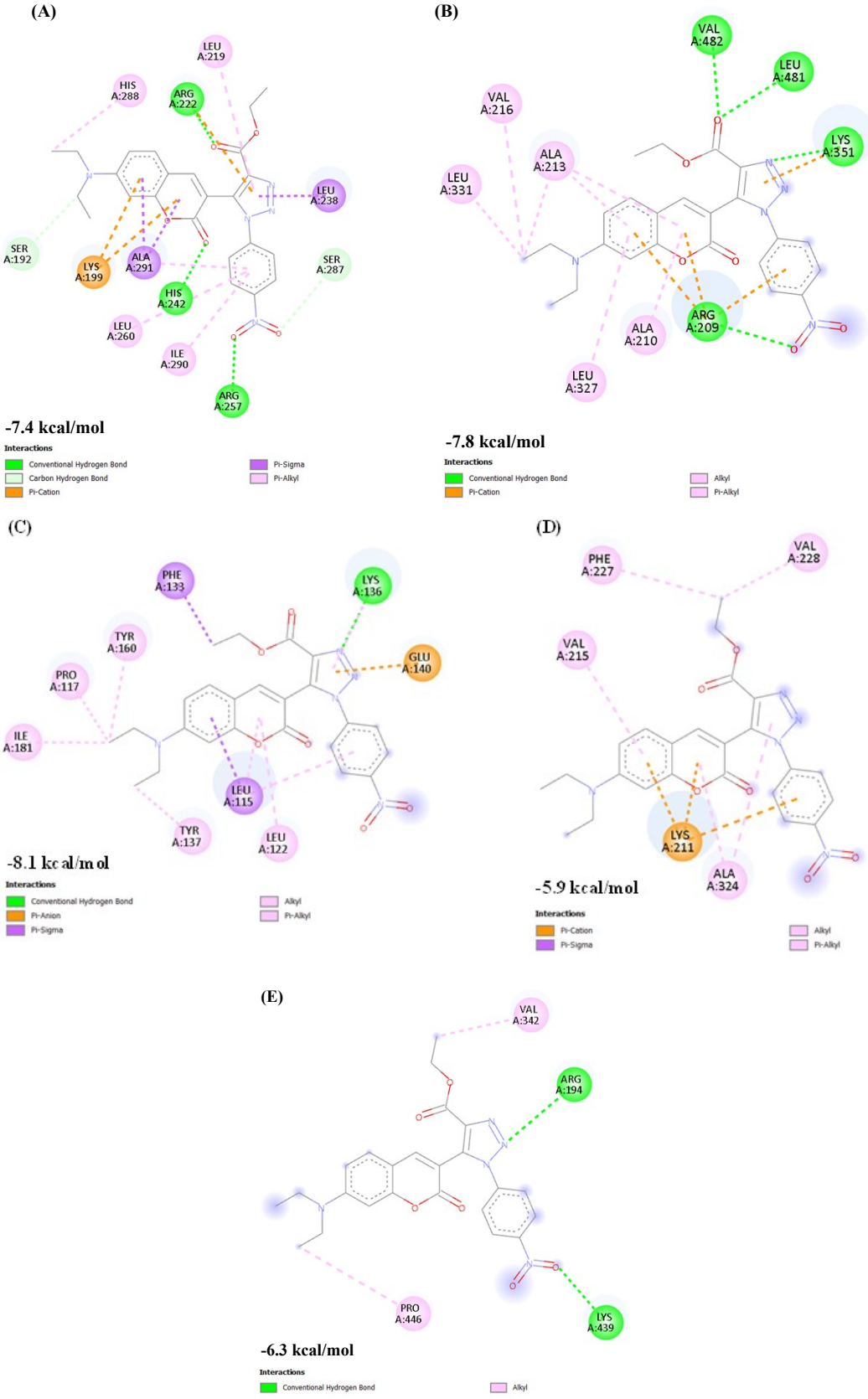

Fig. S26. 2-D view of amino acid residues surrounding **3f** for HSA (A) subdomain IIA (warfarin site) (PDB ID: 2BXD), (B) subdomain IIIA (ibuprofen site) (PDB ID: 2BXG), and for BSA (PDB ID: 4F5S) (C) subdomain IB (bilirubin site) (D) subdomain IIA (warfarin site), (E) subdomain IIIA (ibuprofen site).

13. Molecular Docking Study

14. Table S5: Amino acid residue involved in the ligand-protein interaction and free binding energy

Receptor	Pocket location	Binding affinity of the best docked pose (kcal/mol)	Interacting protein residues	Nature of interaction
HSA	Subdomain IB	-9.8	LEU115, ARG117, PRO118, ILE142, ARG145, PHE149, LEU185, ARG 186	H-bond, Alkyl, π-Alkyl, π -Sigma
	Subdomain IIA	-7.4	SER192, LYS199, LEU219, ARG222, LEU238, HIS242, ARG257, LEU260, SER287, HIS288, ILE290, ALA291	H-bond, π-Cation, π-Alkyl, π -Sigma
	Subdomain IIIA	-7.8	ARG209, ALA210, ALA213, VAL216, LEU327, LEU331, LYS351, LEU481, VAL482	H-bond, Alkyl, π-Cation, π -Alkyl
BSA	Subdomain IB	−8.1	LEU115, PRO117, LEU122, PHE133, LYS136, TYR137, GLU140, TYR160, ILE181	H-bond, Alkyl, π-anion, π-Alkyl, π -Sigma
	Subdomain IIA	-5.9	LYS211, VAL215, PHE227, VAL228, ALA324	π-Cation, π-Alkyl, π -Sigma, π -Alkyl
	Subdomain IIIA	-6.3	ARG194, VAL342, LYS439, PRO446	H-bond, Alkyl

15. HSA detection in a real urine sample and paper strip experiment

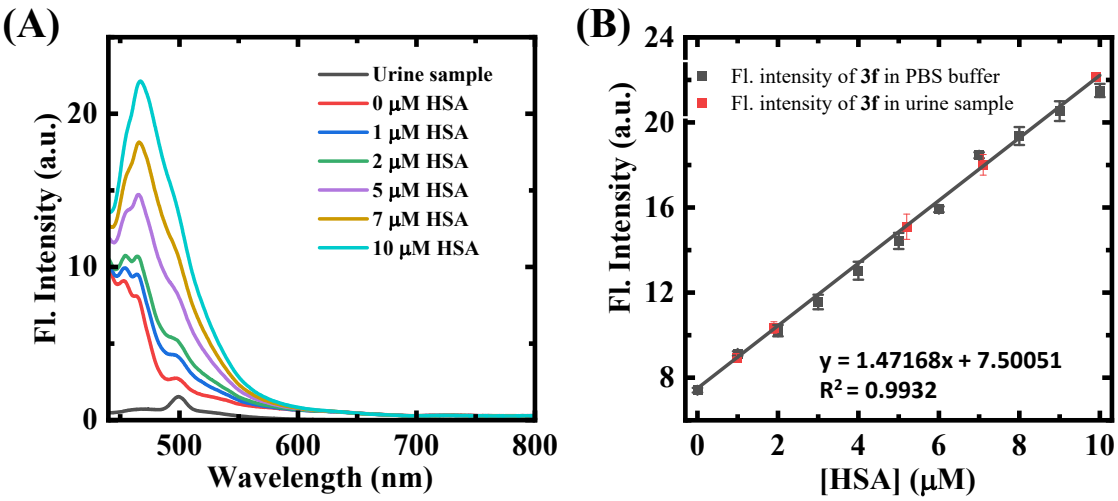

Fig. S27. (A) Emission intensity of **3f** (20 μM, λ_{ex} = 425 nm) upon addition of HSA (0-10 μM) in diluted urine (50-fold dilution) in phosphate buffer solution (pH = 7.4) at 25°C; (B) Calibration plot of emission intensity of **3f** with HSA concentration added in a buffer containing 10 mM Na_2HPO_4 (pH = 7.4) at 25°C. Error bars: (±SD, n=3).

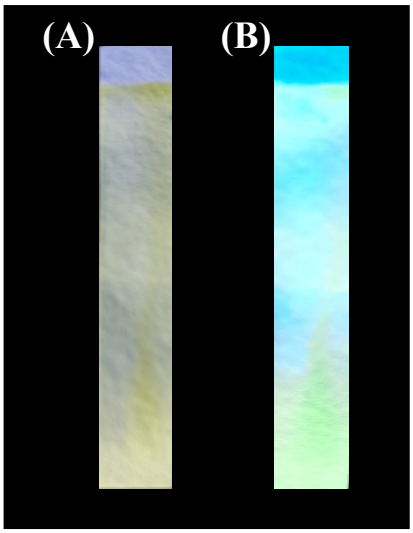

Fig. S28. (A) **3f**-coated filter paper treated with blank diluted urine sample; (B) **3f**-coated filter paper treated with HSA-spiked diluted urine sample in a buffer containing 10 mM Na_2HPO_4 (pH = 7.4) at 25 °C.